Cell death and mitochondrial dysfunction induced by the dietary non-proteinogenic amino acid L-azetidine-2-carboxylic acid (Aze)

Kate Samardzic and Kenneth J. Rodgers
Neurotoxin Research Group
School of Life Sciences
University of Technology Sydney
Australia

Address correspondence to: A/Prof. Ken Rodgers, School of Life Sciences (04.06.340),

University of Technology, Harris Street, Sydney,

NSW 2007 Australia; Tel: +61-2-9514-8373

Fax: +61-2-9550-3302; E-mail: kenneth.rodgers@uts.edu.au

Acknowledgements: Centre for Health Technologies, University of Technology Sydney

Abstract: In addition to the 20 protein amino acids that are vital to human health, hundreds of naturally occurring amino acids, known as non-proteinogenic amino acids (NPAAs) exist and can enter the human food chain. Some NPAAs are toxic through their ability to mimic protein amino acids and this property is utilised by NPAA-containing plants to inhibit the growth of other plants or kill herbivores. The NPAA L-azetidine-2-carboxylic acid (Aze) enters the food chain through the use of sugar beet (*Beta vulgaris)* by-products as feed in the livestock industry and may also be found in sugar beet by-product fibre supplements. Aze mimics the protein amino acid L-proline and readily misincorporates into proteins. In light of this we examined the toxicity of Aze to mammalian cells *in vitro*. We showed decreased viability in Aze exposed cells with both apoptotic and necrotic cell death. This was accompanied by alterations in endosomal-lysosomal activity, changes to mitochondrial morphology and a significant decline in mitochondrial function. In summary, the results show that Aze exposure can lead to deleterious effects on human neuron-like cells and highlight the importance of monitoring human Aze consumption via the food chain.

Keywords: non protein amino acid; azetidine-2-carboxylic acid; mitochondria; multiple sclerosis

1. Introduction

Hundreds of non-proteinogenic amino acids (NPAAs) exist in nature and fulfil diverse biological roles. Less common than their protein amino acid counterparts, yet more abundant, NPAAs have historically been overlooked in favour of research into the biological roles of the protein encoded amino acids. As secondary metabolites in plants, NPAAs are not essential to normal growth, development or reproduction. In fact, in some cases, their role in plants is much more sinister and NPAAs are thought to have evolved to protect plants from the attacks of predators, pathogens or to adversely affect competing plants (Bertin et al. 2007; Rosenthal 2001). This phenomenon arises from the structural similarity of some NPAAs to protein amino acids and as such, they are termed amino acid analogues (Thompson et al. 1969). NPAAs that are known to inhibit biological processes are close structural analogues of protein amino acids. This structural similarity to their respective corresponding protein amino acids has been attributed to their toxicity through a process dubbed protein 'misincorporation' or amino acid 'mimicry' (Song et al. 2017) where the NPAAs are mistakenly utilised in protein synthesis with the error resulting in potentially deleterious effects (Rodgers and Shiozawa 2008; Dunlop et al. 2011). Several other amino acid analogues have been shown to misincorporate in place of their parent amino acid (Rodgers and Shiozawa 2008) and among them is the NPAA L-azetidine-2-carboxylic acid (Aze) (Alescio 1973). Misincorporation is a random process in which the NPAA competes with a protein amino acid for charging to the transfer RNA (Rodgers 2014). The NPAA can then be inserted into any newly synthesised proteins encoded for that protein amino acid provided it can by-pass the proof-reading process (Song et al. 2017).

Aze is produced by sugar beets (*Beta vulgaris*) and lilies (*Convallaria majalis*) and is a structural analogue of the protein encoded amino acid L-proline (Fig 1) (Fowden 1956, 1972). While the Aze containing lily also contains acutely toxic cardiac glycosides and therefore eschews human consumption (Löffelhardt et al. 1979), sugar beets do provide an avenue for human exposure to Aze. Even though sugar beets themselves are rarely consumed in quantities that would warrant concern over Aze exposure, over 250 million tonnes of sugar beets are grown annually worldwide (FAO 2014). Such large quantities are demanded due to the role of sugar beets as the starting material for approximately 20% of the world's commercial sugar production (FAO 2014). Aze containing by-products of this process, known as sugar beet pulp or fibre, are used primarily as feed for livestock and as human dietary fibre supplements (Harland et al. 2009; Golini et al. 2017; Habeeb et al. 2017). In addition to concerns over direct human exposure, humans may be indirectly exposed to Aze through bioaccumulation in dairy and meat products (Rubenstein et al. 2009). In 2006, Rubenstein et al. detected Aze in four varieties of garden beets at a ratio of 1-5 % Aze to L-proline, which based on the current US National Nutrient Database findings would relate to 0.49 – 2.45 mg Aze per cup (246 g) of beets consumed (Rubenstein et al. 2006; Agriculture 2019). In 2009, Rubenstein et al. also quantified Aze concentration in sugar beet by-products, detecting up to 0.34 mg/ 100mg (Rubenstein et al. 2009).

Since Aze was first discovered in plants in the 1950s, there has been much speculation about its ability to mimic protein amino acids and thereby exert a toxic effect in humans. A known plant toxin, the ability of Aze to

incorporate in place of L-proline has been shown in multiple plant models (Vaughan et al. 1974; Lee et al. 1996). In addition, Lee et al. found that 5 mM Aze treatment induced a heat shock-like response (Lee et al. 1996), which is often produced by cells in response to abnormal protein synthesis (Rodgers et al. 2009). Aze incorporates into the L-proline rich myelin basic protein of *Escherichia coli* (*E.coli*) and is toxic to chick embryos due to incorrectly formed collagen, another L-proline rich protein (Bessonov et al. 2010; Lane et al. 1970; Fraser and Deber 1985). These findings are particularly pertinent to humans since the worldwide distribution of the neurodegenerative disorder multiple sclerosis (MS) correlates with regions of high sugar beet production (Poskanzer et al. 1980; Karni et al. 2003; Sarasoja et al. 2004; Beck et al. 2005; Rubenstein 2008). MS is a demyelinating condition and the loss of myelin basic protein function is known to trigger this process. Given that Aze is capable of misincorporating into myelin basic protein and the potential for both direct and indirect human consumption, the present study aims to examine the effect of Aze on the viability and function of human neuroblastoma cells.

2. Materials and Methods

2.1. Reagents

Dulbecco's Modified Eagle's Medium (DMEM), Eagle's Minimal Essential Medium (EMEM, deficient in L-proline) and L-azetidine-2-carboxylic acid were from Sigma Chemical Co., St Louis, MO. All aqueous solutions and buffers were prepared using 18 mU water. All other chemicals and solvents were of cell-culture grade.

2.2. Cell culture

SH-SY5Y human neuroblastoma cells (American Tissue Culture Collection, catalogue number CRL-2266) were cultured as follows; DMEM was supplemented with 10% heat-inactivated Foetal Bovine Serum (FBS) (US origin, Gibco Carlsbad, CA, USA), and 100 X GlutaMAX (Thermo Fisher Scientific, Waltham, MA, USA). Cells were maintained at 37 °C with 5% CO_2 in 175 cm^2 flasks until they were plated for specific experiments. During treatment, DMEM culture medium was substituted with L-proline deficient EMEM. Experiments were performed between passages 17 and 26.

2.3. *Cell viability*

Cells were plated in 96 well plates at 30,000 cells/ well, allowed to adhere overnight, then treated in triplicate with the following concentrations of Aze; 125 µM, 250 µM, 500 µM, 1000 µM and 2000 µM. Cells were treated for 24 h and then incubated with 10% Alamar Blue cell viability reagent (Thermo Fisher) for 2 h. Fluorescence was read at ex 570/em 585. Protein concentration was determined with the bicinchoninic acid (BCA) assay (Smith et al. 1985) and fluorescence was normalised to protein concentration.

2.4. *Live cell imaging cell viability time course*

Cells were plated into 24 well plates at 60,000 cells/well, allowed to adhere overnight, then stained with Hoechst 33258 nuclei stain for 15 min and treated in duplicate with Aze at 500 µM and 2000 µM in EMEM containing propidium iodide (PI) and placed in a microscope heated chamber warmed to 37 °C with 5% CO_2. Images were captured with a high-speed charge-coupled device (CCD) camera using the NIS-Elements acquisition software mounted on a Nikon Ti inverted fluorescence microscope equipped with 20X objective lens (Plan Apo NA 1.4 aperture) and the Perfect Focus System™ for continuous maintenance of focus. Hoechst was monitored with a bandpass 470 emission filter and PI was monitored at emission 636. Time-lapse images were collected every 30 min over a 24 h period with 2 fields of view from each well imaged. Exposure time and brightness/ contrast setting were kept constant for each using the NIS-Elements acquisition software. Images were analysed in FIJI (Schindelin et al. 2012) following background subtraction with a rolling ball radius. PI staining was measured using the mean grey value and fluorescence was normalised to the number of Hoechst positive nuclei.

2.5. *Acidic vesicle activity*

Cells were plated into 24 well plates at 60,000 cells/well, allowed to adhere overnight, and then stained with Hoechst 33258 nuclei stain as above. The acidotropic dye LysoTracker Red DND-99 was then diluted in EMEM containing Aze at 2000 µM and added to wells in triplicate. The plate was then placed in a microscope heated chamber warmed to 37 °C with 5% CO_2 and images were then captured using the Nikon Ti and NIS-Elements at emission 470 for Hoechst 33258 and emission 636 for LysoTracker Red DND-99. Time-lapse images were collected every 30 min over a 24 h period with 2 fields of view from each well imaged. Exposure time and brightness/ contrast setting were kept constant for each using the NIS-Elements acquisition software. Images were analysed in FIJI following background subtraction with a rolling ball radius. Acid vesicle intensity was measured using the mean grey value of LysoTracker uptake and fluorescence was normalised to the number of Hoechst positive nuclei.

2.6. *Cathepsin B activity*

The activity of the lysosomal cysteine protease cathepsin B (CatB) was measured by the linear increase in fluorescence following the cleavage of 7-amino-4-methylcoumarin (AMC) from the peptide substrate Z-Arg-Arg-AMC (where z is benzyloxycarbonyl) (as described in (Dunlop et al. 2008)). Briefly, cells were subcultured onto 6 well plates at 400,000 cells/well and treated in triplicate with 2000 µM Aze in EMEM for 24 h. Cultures were washed three times in phosphate buffered saline (PBS) and harvested by scraping into 200 µL of cathepsin assay buffer (0.1 M phosphate buffer (pH 6) containing 5 mM EDTA, 0.005% Brij 30, 1 µM pepstatin A and 5 mM benzamidine). Cells underwent three freeze/thaw cycles and then lysates were centrifuged at 10,000 x g for 10 min to remove particulates. A 20 µL aliquot of the supernatant, was activated with dithiothreitol (DTT) (final concentration 2.5 mM) and assay buffer were added, in triplicate, to a 96 well plate. Following addition of 50 µM substrate, changes in fluorescence (ex 360/em 460) were measured every 1 min for 29 min. Results were normalised to protein concentration using a BCA assay and activity was expressed as the change in fluorescence over time ($\Delta F/t$).

2.7. *Apoptotic activity*

The apoptotic activity of cells was determined using the Annexin V-fluorescein isothiocyanate (FITC) Apoptosis Detection Kit (Abcam, Cambridge, UK) as recommended by the manufacturer. Cells were plated into 24 well plates at 60,000 cells/well, allowed to adhere overnight, and then stained with Hoechst 33258 nuclei stain as above. The Annexin V-FITC was then diluted in EMEM containing Aze at 2000 µM and added to wells in duplicate. The plate was then placed in a microscope heated chamber warmed to 37 °C with 5% CO_2 and images were then captured as above.

2.8. *Mitochondrial Morphology*

To examine mitochondrial morphology, cells were seeded on sterile glass coverslips that were placed in 12 well plates. The next day, the cells were treated with 2000 µM Aze. At 24 h post treatment, the cells were fixed with 2% paraformaldehyde for 20 min, quenched in 100 mM glycine for 5 min, blocked in 2% bovine serum albumin (BSA) in PBS for 1 h, permeabilised in 0.5% Triton X-100 for 5 min and incubated with mitochondrial mouse monoclonal antibody MTC02 (Abcam) overnight at 4°C. Next, the cells were incubated with a mouse secondary antibody conjugated to CF488A for 1 h at RT in the dark, followed by 4',6-diamidino-2-phenylindole (DAPI) nucleic acid stain (Thermo Fisher) for 5 min. Slides were then prepared with one drop of Dako and sealed using nail varnish. Images were obtained at 60X using a DeltaVision Elite microscope and the DAPI and FITC channels. Images were analysed in FIJI using the macro Mito-Morphology (Dagda et al. 2009). Briefly, the green channel of cells stained with the anti-mitochondria antibody was extracted to greyscale, inverted to show mitochondria-specific fluorescence as black pixels, and thresholded to optimally resolve all individual mitochondria per cell. The macro traced mitochondrial outlines using “analyse particles.” The area measurement refers to the average area of all mitochondria analysed per cell and the mean area/perimeter ratio was employed as an index of mitochondrial interconnectivity. Mitochondrial elongation was measured as inverse circularity. For each condition, a total of 81 cells were measured from three independent experiments (27 each).

2.9. *Mitochondrial Bioenergetics*

A mitochondrial bioenergetics analysis was performed by measuring the oxygen consumption rate (OCR) of cultured cells using the Seahorse XFe24 Extracellular Flux analyser (Agilent, Santa Clara, CA, USA). Cells were plated at 30,000 cells/ well and left overnight to adhere. Cells were then treated with Aze at 2000 μM for 24 h. The Mito Stress Test (Agilent) was then performed according to manufacturer's instructions. Cells were then washed in Seahorse assay media and prepared using the manufacturer's protocol and kit reagents (oligomycin (1 μM), FCCP (1 μM) and antimycin A/rotenone (0.5 μM)). OCR values were normalised to protein concentration using the BCA assay. Basal respiration, maximal respiration, ATP production and non-mitochondrial respiration were then calculated using the Seahorse XF Cell Mito Stress Test Report Generator. Calculations are as follows; non-mitochondrial respiration equates to the minimum rate measurement after antimycin A/rotenone injection, basal respiration equates to last rate measurement before oligomycin injection subtracted from non-mitochondrial respiration, maximal respiration equates to maximum rate measurement after FCCP injection subtracted from non-mitochondrial respiration and ATP production equates to last rate measurement before oligomycin injection subtracted from the minimum rate after oligomycin injection.

2.9.1. Statistical Analysis

Statistical analyses were evaluated using GraphPad software (CA, USA) Prism 7 version 7.03 using either one or two-way ANOVA with Dunnett's multiple comparison post-tests to compare replicate means between different treatments across the samples or Welch's t-test. Differences were considered significant at $P < 0.05$.

3. Results

3.1. Exposure of SH-SY5Y cells to Aze caused a decrease in cell viability

Cell viability was assessed in SH-SY5Y cells over a range of Aze concentrations for 24 h using the Alamar Blue assay (Fig 2A). Cell viability was unchanged at concentrations up to 1000 μM Aze but decreased to 65 % at 2000 μM Aze ($P < 0.0001$).

3.2. Time-course of Aze-induced necrosis in live cells

In order to determine the time-course of Aze induced toxicity we examined the uptake of PI on live cells treated with Aze (500 and 2000 μM) over a 24 h period (Fig 2B). PI uptake is indicative of irreversible cell membrane damage and necrotic cell death. At 2000 μM Aze there were significant increases in PI uptake relative to untreated cells after 12 h, 18 h ($P < 0.05$) and 24 h ($P < 0.01$). An increase in necrotic cell death relative to the control cells was not seen in cells treated with 500 μM Aze. The full time course and representative images are included within the Electronic Supplementary Material (supplementary Fig 1 & 2)

3.3. Lysotracker intensity is increased by Aze exposure while lysosomal protease CatB activity decreased

The fluorescence intensity of acidic bodies in the cell was monitored over 24 h of exposure to 2000 μM Aze using the dye LysoTracker Red DND-99. Fluorescence microscopy was used to visualise the acidic vesicles (supplementary Fig 3) and fluorescence intensity of the images was then analysed using the software FIJI (Fig 2C). Aze treatment significantly increased Lysotracker intensity compared to the untreated cells after 18 h ($P < 0.01$) and 24 h ($P < 0.0001$). CatB activity was measured directly through the cleavage of a fluorescent substrate peptide (Fig 2E) and small but signficant decrease in activity was observed in cells treated with 2000 μM Aze for 24 h ($P < 0.0001$).

3.4. Aze exposure leads to apoptotic cell death

The apoptotic activity of cells was monitored over 24 h of Aze (2000 μM) treatment using Annexin V-FITC. Fluorescence microscopy and FIJI software were used to visualise and analyse fluorescence (Fig 2D). The fluorescence intensity of Annexin V-FITC was significantly increased 18 and 24 h after Aze treatment (P <

0.0001), indicating an increase in apoptotic cell death. Representative images are included in the Electronic Supplementary Material (supplementary Fig 4).

3.5. Aze induces morphological changes to mitochondria

Mitochondrial morphology following treatment with Aze at 2000 µM was assessed using fluorescence microscopy (Fig 3A-D). Morphological changes pertaining to mitochondrial shape, size and connectivity were quantified using FIJI software and the macro Mito Morphology. Following Aze treatment the number of mitochondria per cell significantly decreased by 13.1% ($P < 0.05$) (Fig 4A) and mitochondrial area decreased by 17.7% ($P < 0.001$) (Fig 4B). The mitochondrial elongation score was not affected (Fig 4C) and mitochondrial interconnectivity significantly decreased by 6.6% ($P < 0.001$) (Fig 4D).

3.6. Mitochondrial bioenergetics are affected by Aze treatment

Mitochondrial bioenergetics were analysed by measuring OCR after 24 h of Aze treatment at 2000 µM (Fig 5A). Basal respiration (Fig 5B), which is the oxygen consumption used to meet cellular adenosine triphosphate (ATP) demand under baseline conditions, was significantly decreased by 19.8% ($P < 0.05$). Maximal respiration (Fig 5C), which is the maximal oxygen consumption rate attained following addition of the uncoupler FCCP, decreased by 20.7% ($P < 0.001$). ATP production is derived from the decrease in oxygen consumption following oligomycin injection and shows the portion of basal respiration used to drive mitochondrial ATP production. This was also significantly affected with a decrease of 21.5% ($P < 0.05$) (Fig 5D). The oxygen consumption that persists following antimycin A/ rotenone injection, termed non-mitochondrial respiration, was unaffected (Fig 5E).

4. Discussion

In the present studies we observed significant decreases in SH-SY5Y cell viability after exposure to 2000 µM Aze for 24 h (Fig 2A). The toxicity was similar to that previously reported in HeLa cells (Song et al. 2017) and it is worthwhile noting that in the study by Song et al. the toxicity induced by 5000 µM Aze was rescued using the structural analogue L-proline at 1000 µM but protein amino acids with no structural similarity to L-proline did not provide any protection (Song et al. 2017). A cell viability time course, employing continuous live cell imaging, demonstrated Aze toxicity in mammalian cells as early as 12 h of Aze treatment (Fig 2B). In a similar study by Roest et al. much higher concentrations (10-25 mM) of Aze were required to induce cell death in HeLa cells at similar timepoints (Roest et al. 2018). The previously reported length of time required for Aze incorporation in *E. coli* was 3 h (Grant et al. 1975). Mammalian cell studies using the NPAA beta-methylamino-L-alanine (BMAA) reported an exponential increase in protein bound ^{3}H BMAA within 9 and 16 h treatment periods and this was accompanied by apoptotic but not necrotic cell death (Main et al. 2018; Dunlop et al. 2013).

Our data are consistent with a delayed cytotoxic response due to the synthesis and accumulation of non-native proteins. Aze is a weak competitor for prolyl aminoacyl-tRNA synthetase and can become randomly incorporated into newly synthesised proteins (Rodgers and Shiozawa 2008). The consequences of this could be loss of protein function or alteration in protein structure. In some cases, misfolded proteins are rapidly degraded but they can also resist degradation and form aggregates; possibly through the interaction of exposed hydrophobic regions (Dunlop et al. 2008). Protein aggregates are known to be cytotoxic (Bucciantini et al. 2002). Significant conformational changes to protein structure are caused by Aze insertion, and these are discussed in detail elsewhere (Zagari et al. 1990; Zagari et al. 1994; Rubenstein 2008). Interestingly, Aze-containing peptides may be oxygenated by prolyl hydroxylases resulting in potential damage of the protein by a reverse aldol of the hydroxyazetidine (Liu et al. 2015), contributing further to the deleterious effects of Aze. Despite the low rate of Aze for L-proline substitution, adverse effects of Aze have been reported in plants (Fowden 1963; Verbruggen et al. 1992; Lee et al. 2016a), algae (Kim et al. 2006) and *in vivo* models (Lane et al. 1970; Rojkind 1973; Joneja 1981) and occur even in the presence of normal L-proline production (Fichman et al. 2015).

Since Aze can be incorporated into certain proteins in place of L-proline we then examined the cells to determine if they were responding to an increased load of non-native proteins. Consistent with this, the fluorescence

intensity of acidic vesicles detected by the Lysotracker dye significantly increased following 18 h of Aze treatment when compared to control cells (Fig 2C). A further increase was observed after 24 h exposure. The accumulation of the Lysotracker dye represents expansion of acidified compartments such as late endosomal or lysosomal organelles (Huotari and Helenius 2011). As one of the major systems for the degradation of misfolded proteins, protein aggregates or damaged organelles (Ciechanover and Kwon 2015), an increase in the activity of the endosomal-lysosomal system may be in response to proteins containing misincorporated Aze. The activity of the lysosomal protease CatB however showed a small but significant decrease following Aze treatment (Fig 2E). It has previously been reported that the activity of the lysosomal proteinases can be adversely affected by the rapid delivery of damaged or aggregated proteins to the endosomal-lysosomal system (Rodgers et al. 2004). Cells can then respond by an increase in cathepsin delivery to lysosomes resulting in a rapid increase in lysosomal protease activity (Rodgers et al. 2004). Inhibition of cathepsins has previously been shown to increase Lysotracker staining due to the accumulation of immature cathepsins, reducing the degradative ability of lysosomes and resulting in apoptosis (Jung et al. 2015). Jung et al reported an increase in the levels of the autophagy marker lipidated microtubule-associated protein light-chain 3 (LC3-II), independent of cathepsin activation, which is consistent with previous findings that Aze treatment elevates LC-II (Roest et al. 2018). We hypothesise that the accumulation of misfolded Aze-containing proteins impairs lysosomal function and this can also contribute to cell death.

To examine if programmed cell death played a role in the decline in viability we observed, cells were stained with the apoptosis marker Annexin V. On treatment with Aze the intensity of Annexin V staining gradually increased, and was significantly elevated after 18 h (Fig 2D). Annexin V positive cells were previously observed following 12 h treatment with 2500 μM Aze in primary fibroblasts (Gu et al. 2004). Cross-talk between the endosomal-lysosomal system and apoptotic pathway often occurs following endoplasmic reticulum (ER) stress and ER stress can induce both autophagy and apoptosis (Nikoletopoulou et al. 2013; Ding et al. 2007). Although the present study did not investigate ER stress, Gu et al. used Aze to induce ER stress (Gu et al. 2004) and additionally, Roest et al. recently found that Aze activates both the protein kinase RNA-like ER kinase (PERK) and activating transcription factor 6 (ATF6) arms of the unfolded protein response (Roest et al. 2018). Other NPAAs are also known to induce ER stress (Okle et al. 2013; Jin et al. 2010; Main et al. 2016). Furthermore, ER stress occurs in response to the formation of misfolded proteins and is a common feature of neurodegenerative disorders (Hoozemans and Scheper 2012).

Mitochondria play a key role in the regulation of apoptosis, and dysfunctional mitochondria have been linked to a number of disease pathologies, including neurodegenerative disease (Witte et al. 2014; Su et al. 2010; Wang et al. 2014). In the present studies we detected changes to mitochondrial numbers, area and interconnectivity. The observed decreases in size and interconnectivity are consistent with the formation of mitochondrial fragments during apoptosis, a process facilitated by the mitochondrial fission machinery (Youle and Karbowski 2005; Parone and Martinou 2006). While mitochondrial fragmentation occurs in many forms of apoptosis, damage to mitochondrial proteins may also contribute to the induction of apoptosis. Lee et al. reported that cells depleted of the fusion protein mitofusin 1 were more susceptible to fragmentation and apoptosis upon toxin exposure (Lee et al. 2016b). Furthermore, inhibition of the antiapoptotic mitochondrial protein Bcl-2 is known to induce apoptosis (Mallick et al. 2016). Mitochondria are comprised of around 1000 proteins that, with the exception of 13, are nuclear encoded, translated in the cytosol and the precursor proteins imported into the mitochondria (Backes and Herrmann 2017). The imported proteins generally require proteolytic processing and chaperone assisted folding before they can assume their native conformation (Backes and Herrmann 2017). Even intermittent protein misfolding as could occur due to Aze-incorporation could cause proteotoxic stress in the mitochondria and cause morphological changes as observed in the present studies. Proteins synthesised in the mitochondria may also be more susceptible to NPAA incorporation due to inherent differences in their proofreading machinery, aminoacyl-tRNA synthetases, and NPAA induced mitochondrial protein instability has previously been demonstrated by Konovalova et al. using L-canavanine, an NPAA present in jack beans and wild potato (Suzuki et al. 2011; Konovalova et al. 2015). In addition to fragmentation, the number of mitochondria per cell also decreased. Reductions in mitochondrial numbers have also been observed in cultured mouse neurons expressing a frontotemporal dementia-related tau mutation, suggesting decreased mitochondrial numbers may be associated with early stage development of the disease (Rodríguez-Martín et al. 2016).

Basal and maximal respiration were significantly decreased following Aze treatment, as was ATP production (Fig 5). Protein dysfunction in the respiratory chain could contribute to this decrease, and of the 13 proteins encoded by mitochondria, the L-proline rich ATP synthase protein 8 (Complex V subunit) might be particularly susceptible to misincorporation with 16.2% L-proline content (The UniProt 2018). Mitochondrial bioenergetic collapse is also a well characterised marker of apoptotic and necrotic cell death (Skulachev 2006; Izyumov et al. 2004). While it is clear Aze exposure induces apoptosis, the exact cellular events that precede this downstream response remain unknown. While ER stress has previously been mentioned as one potential apoptosis evoking event, DNA damage, oxidative stress and damage to mitochondrial proteins are also events that warrant investigation in the future (Roos and Kaina 2006; Chandra et al. 2000). This is the first study to show that Aze causes mitochondrial dysfunction and is especially important given the link between mitochondrial dysfunction, apoptosis and neurodegenerative disease, in particular MS (Dutta et al. 2006; Mahad et al. 2008; Mahad et al. 2009).

The results of the present study are particularly pertinent given that the production of Aze containing sugar beets has been historically linked to the development of MS and it has been been hypothesised that Aze misincorporation may trigger the onset of MS in genetically predisposed individuals (Rubenstein 2008). MS is an autoimmune demyelinating disease of the central nervous system and came to prominence in the middle 19th century, some 50 years after the popularisation of sugar beet production (Loma and Heyman 2011; Rubenstein 2008; Murray 2009). In the same way that a neurodegenerative disorder known as amyotrophic lateral sclerosis-Parkinson's dementia complex has been linked to exposure to the cyanotoxic NPAA BMAA on Guam and has been proposed to have contributed to clusters of amyotrophic lateral sclerosis in New Hampshire (Caller et al. 2012), cases of MS are increased in areas that produce sugar beets. In Canada, the region at the centre of the Canadian sugar beet industry coincides with the highest incidence of MS in the country (Beck et al. 2005). Similarly, the Japanese region of Tokachi has the highest MS prevalence in Asia (Houzen et al. 2008). Tokachi also produces 45% of Japan's sugar beets (Rubenstein 2008). This pattern of high MS incidence in synchrony with sugar beet producing regions has also been observed in Sardinia, Scotland's Orkney Islands, the Middle East and Finland (Pugliatti et al. 2001; Poskanzer et al. 1980; Karni et al. 2003; Sarasoja et al. 2004). Although the present studies do not provide direct evidence of a link between Aze exposure and MS, the spectrum of *in vitro* toxicity identified suggests that it has the potential to damage the human nervous system. Further studies investigating levels of human exposure to Aze and its *in vivo* effects would be justified.

5. Conclusions

Aze is toxic to human neuron-like cells and induced mitochondrial damage that is accompanied by an increase in apoptotic. The toxicity observed in this study is important because Aze-containing sugar beets are grown in over 40 countries for the production of sugar (Geng and Yang 2015), and this is set to increase as sugar beets become a source of biofuels such as ethanol (Haankuku et al. 2015). Furthermore, there is significant potential for Aze to enter the human food chain and elicit harmful effects.

6. Compliance with Ethical Standards

1. Disclosure of potential conflicts of interest

Funding: This study was partly funded by the Centre for Health Technologies, University of Technology Sydney

2. Research involving Human Participants and/or Animals

This article does not contain any studies with human participants or animals performed by any of the authors.

3. Informed consent

This article does not contain individual participants requiring informed consent.

Figure Legends

Fig 1 Structural representations of the protein amino acid L-proline and the non-proteinogenic amino acid (NPAA) L-azetidine-2-carboxylic acid (Aze)

Fig 2 Effects of Aze treatment on SH-SY5Y neuroblastoma cells: (A) Cells were exposed to a range of Aze concentrations and viability after 24 h was measured using the Alamar Blue assay; (B) Cell viability as a measure of propidium iodide fluorescence intensity measured over 24 h of Aze treatment using live cell imaging; (C) Lysotracker Red DND-9 staining measured over 24 h of Aze treatment using live cell imaging; (D) Annexin V fluorescent intensity measured over 24 h of Aze treatment using live cell imaging; (E) Cathepsin B activity following 24 h treatment with 2000 μM Aze, expressed as a change in fluorescence over time per μg cell protein ($\Delta F/t$). N=3. Error bars show SEM with significance relative to control represented by * $P < 0.05$, ** $P < 0.01$, *** $P < 0.001$, **** $P < 0.0001$

Fig 3 Fluorescence microscopy images (60X magnification) of the effects of 2000 μM Aze on SH-SY5Y cell mitochondria following 24 h treatment. Cells were stained with an anti-mitochondria antibody (green) and nuclei visualised using DAPI (blue). (A) Control; (B) Magnified image of white box in (A); (C) Aze treated cells; (D) Magnified image of white box in (C). Scale bar 10 μm for (A) and (C)

Fig 4 Comparison of mitochondrial morphology in Aze 2000 μM treated SH-SY5Y neuroblastoma cells and control cells after 24 h. (A) Mitochondrial number; (B) Mitochondrial area; (C) Mitochondrial elongation score; (D) Mitochondrial interconnectivity score. N=3. Error bars show SEM with significance relative to control represented by * $P < 0.05$, ** $P < 0.01$, *** $P < 0.001$

Fig 5 Mitochondrial bioenergetics of SH-SY5Y neuroblastoma cells following 2000 μM Aze treatment for 24 h. (A) Oxygen consumption rate (OCR) measured using the Seahorse XFe24 analyser with oligomycin, FFCP and antimycin A/rotenone injections; (B) Basal respiration; (C) Maximal respiration; (D) ATP production; (E) Non-mitochondrial respiration. N=3. Error bars show SEM with significance relative to control represented by * $P < 0.05$, *** $P < 0.001$

References

USDA Food Composition Database (2019).

Alescio T (1973) Effect of a Proline Analogue, Azetidine-2-carboxylic Acid, on the Morphogenesis in vitro of mouse embyronic lung. J Embryol Exp Morphol 29:439-451

Backes S, Herrmann JM (2017) Protein Translocation into the Intermembrane Space and Matrix of Mitochondria: Mechanisms and Driving Forces. Front Mol Biosci 4:83. doi:10.3389/fmolb.2017.00083

Beck CA, Metz LM, Svenson LW, Patten SB (2005) Regional variation of multiple sclerosis prevalence in Canada. Mult Scler J 11 (5):516-519

Bertin C, Weston LA, Huang T, Jander G, Owens T, Meinwald J, Schroeder FC (2007) Grass roots chemistry: meta-Tyrosine, an herbicidal nonprotein amino acid. Proceedings of the National Academy of Sciences of the United States of America 104 (43):16964-16969. doi:10.1073/pnas.0707198104

Bessonov K, Bamm VV, Harauz G (2010) Misincorporation of the proline homologue Aze (azetidine-2-carboxylic acid) into recombinant myelin basic protein. Phytochemistry 71 (5-6):502-507. doi:10.1016/j.phytochem.2009.12.010

Bucciantini M, Giannoni E, Chiti F, Baroni F, Formigli L, Zurdo J, Taddei N, Ramponi G, Dobson CM, Stefani M (2002) Inherent toxicity of aggregates implies a common mechanism for protein misfolding diseases. Nature 416 (6880):507-511. doi:10.1038/416507a

Caller TA, Field NC, J.W C, Shi X, Harris BT, Stommel EW (2012) Spatial clustering of amyotrophic lateral sclerosis and the potential role of BMAA. Amyotroph Lateral Sc 13 (1):25-32

Chandra J, Samali A, Orrenius S (2000) Triggering and modulation of apoptosis by oxidative stress. Free Radic Biol Med 29 (3):323-333. doi:https://doi.org/10.1016/S0891-5849(00)00302-6

Ciechanover A, Kwon YT (2015) Degradation of misfolded proteins in neurodegenerative diseases: therapeutic targets and strategies. Exp Mol Med 47:e147. doi:10.1038/emm.2014.117

Dagda RK, Cherra SJ, 3rd, Kulich SM, Tandon A, Park D, Chu CT (2009) Loss of PINK1 function promotes mitophagy through effects on oxidative stress and mitochondrial fission. J Biol Chem 284 (20):13843-13855. doi:10.1074/jbc.M808515200

Ding WX, Ni HM, Gao W, Hou YF, Melan MA, Chen X, Stolz DB, Shao ZM, Yin XM (2007) Differential effects of endoplasmic reticulum stress-induced autophagy on cell survival. J Biol Chem 282 (7):4702-4710. doi:10.1074/jbc.M609267200

Dunlop RA, Brunk UT, Rodgers KJ (2011) Proteins containing oxidized amino acids induce apoptosis in human monocytes. The Biochemical journal 435 (1):207-216. doi:10.1042/BJ20100682

Dunlop RA, Cox PA, Banack SA, Rodgers KJ (2013) The Non-Protein Amino Acid BMAA Is Misincorporated into Human Proteins in Place of l-Serine Causing Protein Misfolding and Aggregation. PLoS ONE 8 (9):1-6. doi:10.1371/journal.pone.0075376

Dunlop Rachael A, Dean Roger T, Rodgers Kenneth J (2008) The impact of specific oxidized amino acids on protein turnover in J774 cells. Biochemical Journal 410 (1):131

Dutta R, McDonough J, Yin X, Peterson J, Chang A, Torres T, Gudz T, Macklin WB, Lewis DA, Fox RJ, Rudick R, Mirnics K, Trapp BD (2006) Mitochondrial dysfunction as a cause of axonal degeneration in multiple sclerosis patients. Ann Neurol 59 (3):478-489. doi:10.1002/ana.20736

FAO (2014) FAO Statistical Yearbook. In: FAOSTAT (ed)

Fichman Y, Gerdes SY, Kovács H, Szabados L, Zilberstein A, Csonka LN (2015) Evolution of proline biosynthesis: enzymology, bioinformatics, genetics, and transcriptional regulation. Biological Reviews 90 (4):1065-1099. doi:10.1111/brv.12146

Fowden L (1956) Azetidine-2-carboxylic acid: a new cyclic imino acid occurring in plants. The Biochemical journal 64 (2):323-332

Fowden L (1963) Amino-acid Analogues and the Growth of Seedlings. Journal of Experimental Botany 14 (3):387-398. doi:10.1093/jxb/14.3.387

Fowden L (1972) Amino acid complement of plants. Phytochemistry 11 (7):2271-2276. doi:https://doi.org/10.1016/S0031-9422(00)88389-2

Fraser PE, Deber CM (1985) Structure and function of the proline-rich region of myelin basic protein. Biochemistry 24 (17):4593-4598. doi:10.1021/bi00338a017

Geng G, Yang J (2015) Sugar Beet Production and Industry in China. Sugar Tech 17 (1):13-21. doi:10.1007/s12355-014-0353-y

Golini J, Jones WL, Clift IC (2017) The Effect of Increased Fiber Ingestion on Lipid Levels and Body Mass: A 4-Week Trial. J Food Sci Nut 3 (17)

Grant MM, Brown AS, Corwin LM, Troxler RF, Franzblau C (1975) Effect of L-azetidine 2-carboxylic acid on growth and proline metabolism in Escherichia coli. Biochim Biophys Acta 404 (2):180-187

Gu F, Nguyen DT, Stuible M, Dube N, Tremblay M, Chevet E (2004) Protein tyrosine phosphatase 1B potentiates IRE1 signaling during endoplasmic reticulum stress. J Biol Chem 279

Haankuku C, Epplin FM, Kakani VG (2015) Industrial sugar beets to biofuel: Field to fuel production system and cost estimates. Biomass Bioenergy 80:267-277. doi:http://dx.doi.org/10.1016/j.biombioe.2015.05.027

Habeeb AAM, Gad AE, EL-Tarabany A, Mustafa MM, Atta A (2017) Using of Sugar Beet Pulp By-Product in Farm Animals Feeding. IJSRST 3 (3)

Harland JJ, Jones CK, Hufford C (2009) Co-products. In: Draycott AP (ed) Sugar Beet. Blackwell Publishing Ltd, pp 443-463

Hoozemans JJM, Scheper W (2012) Endoplasmic reticulum: The unfolded protein response is tangled in neurodegeneration. Int J Biochem Cell Biol 44 (8):1295-1298. doi:https://doi.org/10.1016/j.biocel.2012.04.023

Houzen H, Niino M, Hata D, Nakano F, Kikuchi S, Fukazawa T, Sasaki H (2008) Increasing prevalence and incidence of multiple sclerosis in northern Japan. Mult Scler J 14 (7):887-892. doi:10.1177/1352458508090226

Huotari J, Helenius A (2011) Endosome maturation. The EMBO journal 30 (17):3481-3500. doi:10.1038/emboj.2011.286

Izyumov DS, Avetisyan AV, Pletjushkina OY, Sakharov DV, Wirtz KW, Chernyak BV, Skulachev VP (2004) “Wages of Fear”: transient threefold decrease in intracellular ATP level imposes apoptosis. Biochim Biophys Acta Bioenerg 1658 (1):141-147. doi:https://doi.org/10.1016/j.bbabio.2004.05.007

Jin CM, Yang YJ, Huang HS, Kai M, Lee MK (2010) Mechanisms of L-DOPA-induced cytotoxicity in rat adrenal pheochromocytoma cells: implication of oxidative stress-related kinases and cyclic AMP. Neuroscience 170 (2):390-398. doi:10.1016/j.neuroscience.2010.07.039

Joneja MG (1981) Teratogenic effects of proline analogue L-azetidine-2-carboxylic acid in hamster fetuses. Teratology 23 (3):365-372. doi:10.1002/tera.1420230311

Jung M, Lee J, Seo H-Y, Lim JS, Kim E-K (2015) Cathepsin Inhibition-Induced Lysosomal Dysfunction Enhances Pancreatic Beta-Cell Apoptosis in High Glucose. PLOS ONE 10 (1):e0116972. doi:10.1371/journal.pone.0116972

Karni A, Kahana E, Zilber N, Abramsky O, Alter M, Karussis D (2003) The Frequency of Multiple Sclerosis in Jewish and Arab Populations in Greater Jerusalem. Neuroepidemiology 22 (1):82-86

Kim J-S, Kim J-C, Lee S, Lee B-H, Cho KY (2006) Biological activity of l-2-azetidinecarboxylic acid, isolated from Polygonatum odoratum var. pluriflorum, against several algae. Aquatic Botany 85 (1):1-6. doi:http://dx.doi.org/10.1016/j.aquabot.2006.01.003

Konovalova S, Hilander T, Loayza-Puch F, Rooijers K, Agami R, Tyynismaa H (2015) Exposure to arginine analog canavanine induces aberrant mitochondrial translation products, mitoribosome stalling, and instability of the mitochondrial proteome. Int J Biochem Cell Biol 65:268-274. doi:http://dx.doi.org/10.1016/j.biocel.2015.06.018

Lane JM, Dehm P, Prockop DJ (1970) Effect of the Proline Analogue Azetidine-2-carboxylic Acid on Collagen Synthesis in vivo. Biochim Biophys Acta 236:517- 527

Lee J, Joshi N, Pasini R, Dobson RC, Allison J, Leustek T (2016a) Inhibition of Arabidopsis growth by the allelopathic compound azetidine-2-carboxylate is due to the low amino acid specificity of cytosolic prolyl-tRNA synthetase. Plant J 88 (2):236-246. doi:10.1111/tpj.13246

Lee W-C, Chiu C-H, Chen J-B, Chen C-H, Chang H-W (2016b) Mitochondrial Fission Increases Apoptosis and Decreases Autophagy in Renal Proximal Tubular Epithelial Cells Treated with High Glucose. DNA Cell Biol 35 (11):657-665. doi:10.1089/dna.2016.3261

Lee YRJ, Nagao RT, Lin CY, Key JL (1996) Induction and Regulation of Heat-Shock Gene Expression by an Amino Acid Analog in Soybean Seedlings. Plant Physiol 110 (1):241-248

Liu Z, Jenkinson SF, Vermaas T, Adachi I, Wormald MR, Hata Y, Kurashima Y, Kaji A, Yu CY, Kato A, Fleet GW (2015) 3-Fluoro-azetidine Carboxylic Acids and trans,trans-3,4-Difluoroproline as Peptide Scaffolds: Inhibition of Pancreatic Cancer Cell Growth by a Fluoroazetidine Iminosugar. The Journal of organic chemistry 80 (9). doi:10.1021/acs.joc.5b00463

Löffelhardt W, Kopp B, Kubelka W (1979) Intracellular distribution of cardiac glycosides in leaves of Convallaria majalis. Phytochemistry 18 (8):1289-1291. doi:https://doi.org/10.1016/0031-9422(79)83009-5

Loma I, Heyman R (2011) Multiple Sclerosis: Pathogenesis and Treatment. Current Neuropharmacol 9 (3):409-416. doi:10.2174/157015911796557911

Mahad DJ, Ziabreva I, Campbell G, Lax N, White K, Hanson PS, Lassmann H, Turnbull DM (2009) Mitochondrial changes within axons in multiple sclerosis. Brain 132 (5):1161-1174. doi:10.1093/brain/awp046

Mahad DJ, Ziabreva I, Lassmann H, Turnbull D (2008) Mitochondrial defects in acute multiple sclerosis lesions. Brain 131 (7):1722-1735. doi:10.1093/brain/awn105

Main BJ, Dunlop RA, Rodgers KJ (2016) The use of l-serine to prevent β-methylamino-l-alanine (BMAA)-induced proteotoxic stress in vitro. Toxicon : official journal of the International Society on Toxinology 109:7-12. doi:http://dx.doi.org/10.1016/j.toxicon.2015.11.003

Main BJ, Italiano CJ, Rodgers KJ (2018) Investigation of the interaction of β-methylamino-l-alanine with eukaryotic and prokaryotic proteins. Amino Acids 50 (3):397-407. doi:10.1007/s00726-017-2525-z

Mallick A, More P, Syed MM, Basu S (2016) Nanoparticle-Mediated Mitochondrial Damage Induces Apoptosis in Cancer. ACS Appl Mater Interfaces 8 (21):13218-13231. doi:10.1021/acsami.6b00263

Murray TJ (2009) The history of multiple sclerosis: the changing frame of the disease over the centuries. J Neurol Sci 277:S3-S8. doi:https://doi.org/10.1016/S0022-510X(09)70003-6

Nikoletopoulou V, Markaki M, Palikaras K, Tavernarakis N (2013) Crosstalk between apoptosis, necrosis and autophagy. Biochim Biophys Acta Mol Cell Res 1833 (12):3448-3459. doi:https://doi.org/10.1016/j.bbamcr.2013.06.001

Okle O, Stemmer K, Deschl U, Dietrich DR (2013) L-BMAA induced ER stress and enhanced caspase 12 cleavage in human neuroblastoma SH-SY5Y cells at low nonexcitotoxic concentrations. Toxicological sciences : an official journal of the Society of Toxicology 131 (1):217-224. doi:10.1093/toxsci/kfs291

Parone PA, Martinou J-C (2006) Mitochondrial fission and apoptosis: An ongoing trial. Biochim Biophys Acta Mol Cell Res 1763 (5):522-530. doi:https://doi.org/10.1016/j.bbamcr.2006.04.005

Poskanzer DC, Prenney LB, Sheridan JL, Kondy JY (1980) Multiple sclerosis in the Orkney and Shetland Islands. I: Epidemiology, clinical factors, and methodology. J Epidemiol Community Health 34 (4):229-239. doi:10.1136/jech.34.4.229

Pugliatti M, Sotgiu S, Solinas G, Castiglia P, Rosati G (2001) Multiple sclerosis prevalence among Sardinians: further evidence against the latitude gradient theory. Neurol Sci 22 (2):163-165. doi:10.1007/s100720170017

Rodgers KJ (2014) Non-protein amino acids and neurodegeneration: The enemy within. Experimental Neurology 253 (0):192-196. doi:http://dx.doi.org/10.1016/j.expneurol.2013.12.010

Rodgers KJ, Ford JL, Brunk UT (2009) Heat shock proteins: keys to healthy ageing? Redox Rep 14 (4):147-153. doi:10.1179/135100009X392593

Rodgers KJ, Hume PM, Dunlop RA, D Dean RT (2004) Biosynthesis and turnover of DOPA-containing proteins by human cells. Free Radic Biol Med 1 (37)

Rodgers KJ, Shiozawa N (2008) Misincorporation of amino acid analogues into proteins by biosynthesis. Int J Biochem Cell Biol 40 (8):1452-1466. doi:http://dx.doi.org/10.1016/j.biocel.2008.01.009

Rodríguez-Martín T, Pooler AM, Lau DHW, Mórotz GM, De Vos KJ, Gilley J, Coleman MP, Hanger DP (2016) Reduced number of axonal mitochondria and tau hypophosphorylation in mouse P301L tau knockin neurons. Neurobiol Dis 85:1-10. doi:https://doi.org/10.1016/j.nbd.2015.10.007

Roest G, Hesemans E, Welkenhuyzen K, Luyten T, Engedal N, Bultynck G, Parys JB (2018) The ER Stress Inducer l-Azetidine-2-Carboxylic Acid Elevates the Levels of Phospho-eIF2α and of LC3-II in a Ca(2+)-Dependent Manner. Cells 7 (12):239. doi:10.3390/cells7120239

Rojkind M (1973) Inhibition of Liver Fibrosis by L-Azetidine-2-carboxylic Acid in Rats Treated with Carbon Tetrachloride. The Journal of Clinical Investigation 52:2451-2456

Roos WP, Kaina B (2006) DNA damage-induced cell death by apoptosis. Trends Mol Med 12 (9):440-450. doi:https://doi.org/10.1016/j.molmed.2006.07.007

Rosenthal GA (2001) L-Canavanine: a higher plant insecticidal allelochemical. Amino Acids 21:319-330

Rubenstein E (2008) Misincorporation of the proline analog azetidine-2-carboxylic acid in the pathogenesis of multiple sclerosis: a hypothesis. J Neuropathol Exp Neurol 67 (11):1035-1040. doi:10.1097/NEN.0b013e31818add4a

Rubenstein E, McLaughlin T, Winant RC, Sanchez A, Eckart M, Krasinska KM, Chien A (2009) Azetidine-2-carboxylic acid in the food chain. Phytochemistry 70 (1):100-104. doi:10.1016/j.phytochem.2008.11.007

Rubenstein E, Zhou H, Krasinska KM, Chien A, Becker CH (2006) Azetidine-2-carboxylic acid in garden beets (Beta vulgaris). Phytochemistry 67 (9):898-903. doi:https://doi.org/10.1016/j.phytochem.2006.01.028

Sarasoja T, Wikström J, Paltamaa J, Hakama M, Sumelahti ML (2004) Occurrence of multiple sclerosis in central Finland: a regional and temporal comparison during 30 years. Acta Neurologica Scandinavica 110 (5):331-336

Schindelin J, Arganda-Carreras I, Frise E, Kaynig V, Longair M, Pietzsch T, Preibisch S, Rueden C, Saalfeld S, Schmid B, Tinevez JY, White DJ, Hartenstein V, Eliceiri K, Tomancak P, Cardona A (2012) Fiji: an open-source platform for biological-image analysis. Nat Methods 9 (7):676-682. doi:10.1038/nmeth.2019

Skulachev VP (2006) Bioenergetic aspects of apoptosis, necrosis and mitoptosis. Apoptosis 11 (4):473-485. doi:10.1007/s10495-006-5881-9

Smith PK, Krohn RI, Hermanson GT, Mallia AK, Gartner FH, Provenzano MD, Fujimoto EK, Goeke NM, Olson BJ, Klenk DC (1985) Measurement of protein using bicinchoninic acid. Anal Biochem 150 (1):76-85. doi:https://doi.org/10.1016/0003-2697(85)90442-7

Song Y, Zhou H, Vo MN, Shi Y, Nawaz MH, Vargas-Rodriguez O, Diedrich JK, Yates JR, Kishi S, Musier-Forsyth K, Schimmel P (2017) Double mimicry evades tRNA synthetase editing by toxic vegetable-sourced non-proteinogenic amino acid. Nat Commun 8 (1):2281. doi:10.1038/s41467-017-02201-z

Su B, Wang X, Zheng L, Perry G, Smith MA, Zhu X (2010) Abnormal mitochondrial dynamics and neurodegenerative diseases. Biochim Biophys Acta Mol Basis Dis 1802 (1):135-142. doi:http://dx.doi.org/10.1016/j.bbadis.2009.09.013

Suzuki T, Nagao A, Suzuki T (2011) Human Mitochondrial tRNAs: Biogenesis, Function, Structural Aspects, and Diseases. Annu Rev Genet 45 (1):299-329. doi:10.1146/annurev-genet-110410-132531

The UniProt C (2018) UniProt: a worldwide hub of protein knowledge. Nucleic Acids Research 47 (D1):D506-D515. doi:10.1093/nar/gky1049

Thompson JF, Morris CJ, Smith IK (1969) New naturally occurring amino acids. Annu Rev Biochem 38 (1):137-158. doi:10.1146/annurev.bi.38.070169.001033

Vaughan D, Dekock PC, Cusens E (1974) Effects of Hydroxyproline and other Amino Acid Analogues on the Growth of Pea Root Segments. Physiol Plant 30 (3):255-259. doi:10.1111/j.1399-3054.1974.tb03652.x

Verbruggen N, van Montagu M, Messens E (1992) Synthesis of the proline analogue [2,3-3H]azetidine-2-carboxylic acid. Uptake and incorporation in Arabidopsis thaliana and Escherichia coli. FEBS letters 308 (3):261-263.

Wang X, Wang W, Li L, Perry G, Lee H-g, Zhu X (2014) Oxidative stress and mitochondrial dysfunction in Alzheimer's disease. Biochim Biophys Acta Mol Basis Dis 1842 (8):1240-1247. doi:https://doi.org/10.1016/j.bbadis.2013.10.015

Witte ME, Mahad DJ, Lassmann H, van Horssen J (2014) Mitochondrial dysfunction contributes to neurodegeneration in multiple sclerosis. Trends Mol Med 20 (3):179-187. doi:https://doi.org/10.1016/j.molmed.2013.11.007

Youle RJ, Karbowski M (2005) Mitochondrial fission in apoptosis. Nat Rev Mol Cell Biol 6 (8)

Zagari A, Nemethy G, Scheraga HA (1990) The Effect of L-Azetidine-2-Carboxylic Acid Residue on Protein Conformation. l. Conformations of the Residue and of Dipeptides. Biopolymers 30

Zagari A, Palmer KA, Gibson KD, Nemethy G, Scheraga HA (1994) The effect of the l-azetidine-2-carboxylic acid residue on protein conformation. IV. Local substitutions in the collagen triple helix. Biopolymers 34 (1):51-60. doi:10.1002/bip.360340107

Figure 1

Click here to access/download;Figure;Slide1.tiff

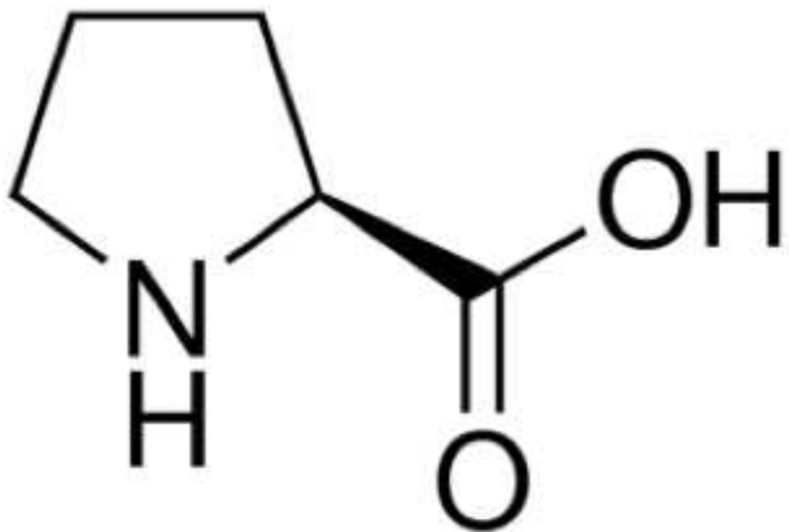

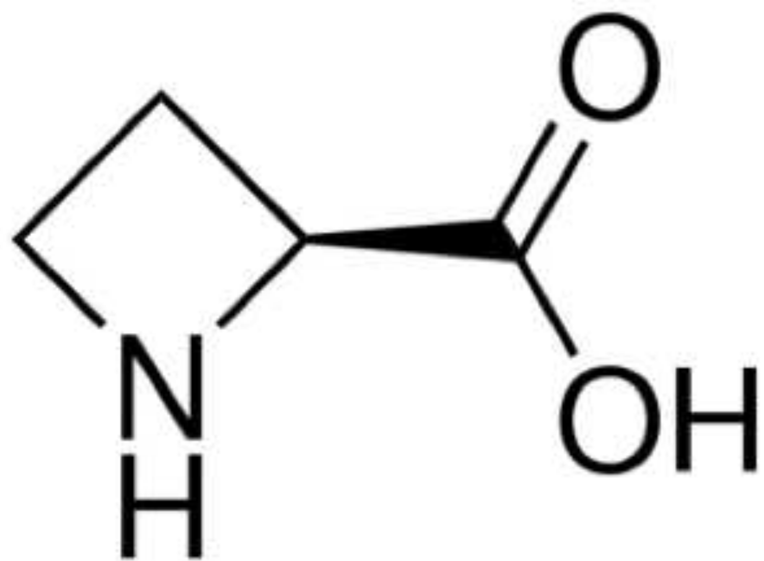

Figure 2

Click here to access/download;Figure;Figure 2 Aze updated.tiff

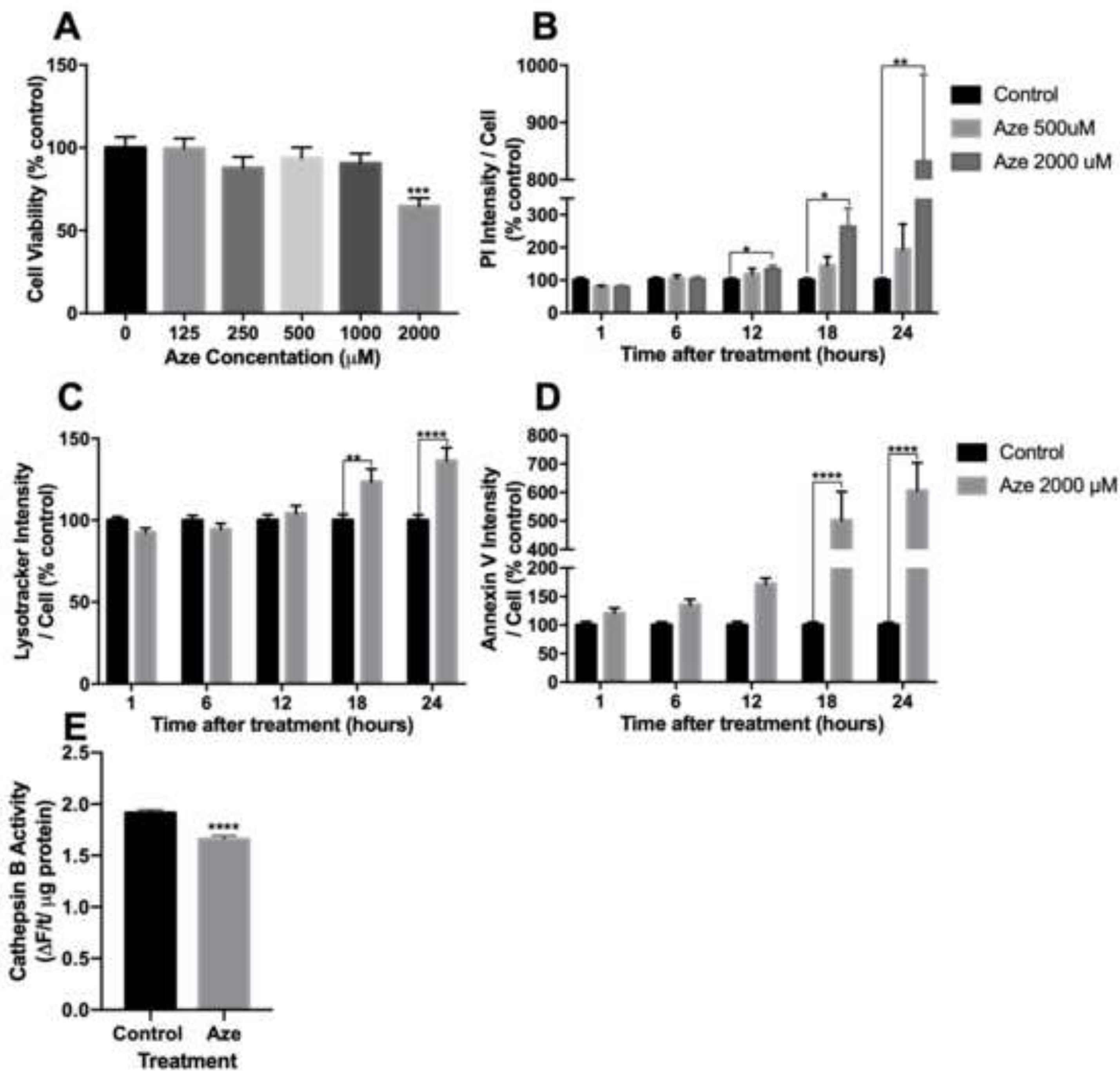

Figure 3

Click here to access/download;Figure;Fig 3b Aze.tif

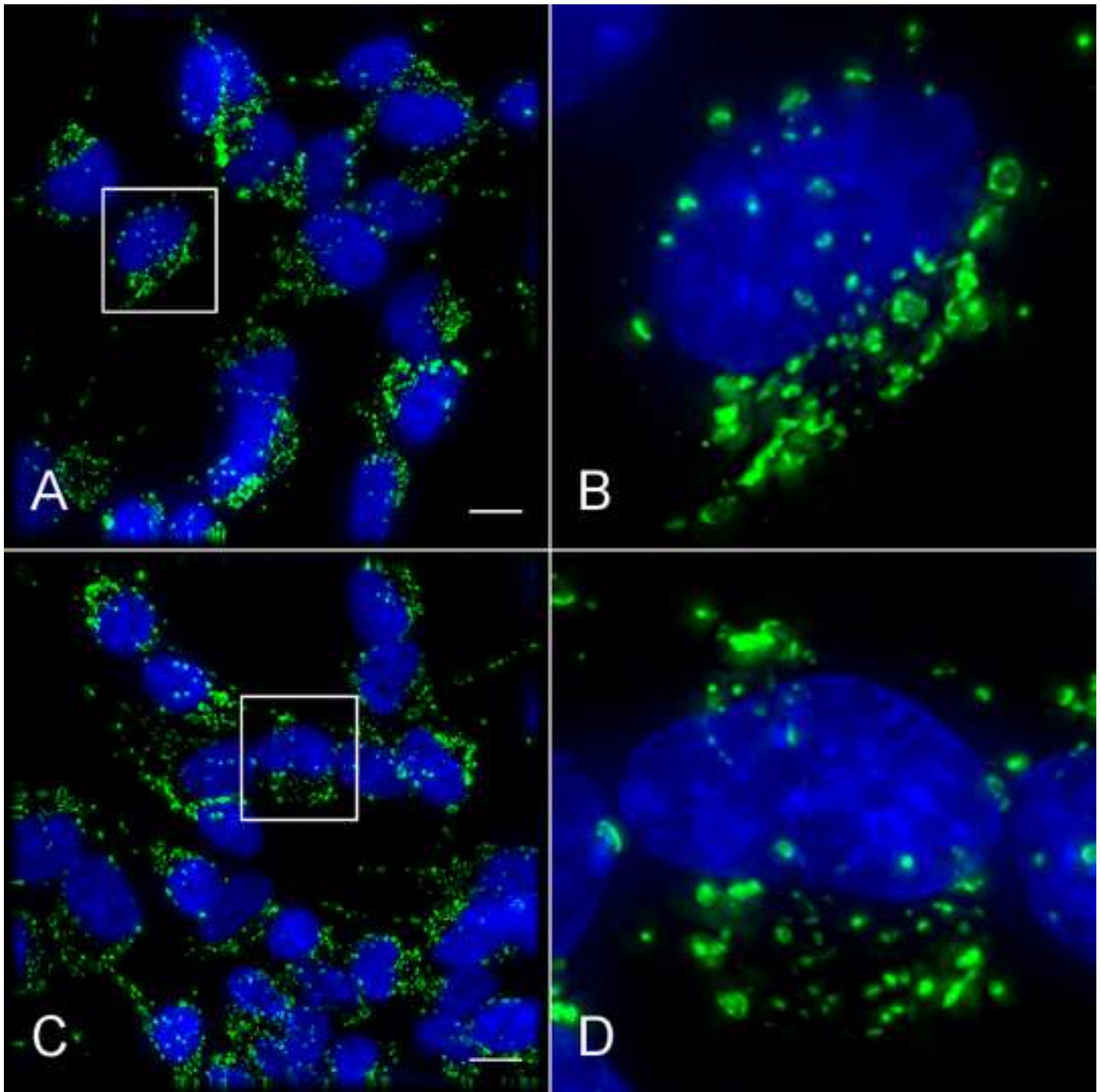

Figure 4

Click here to access/download;Figure;Fig 4 Aze.tif

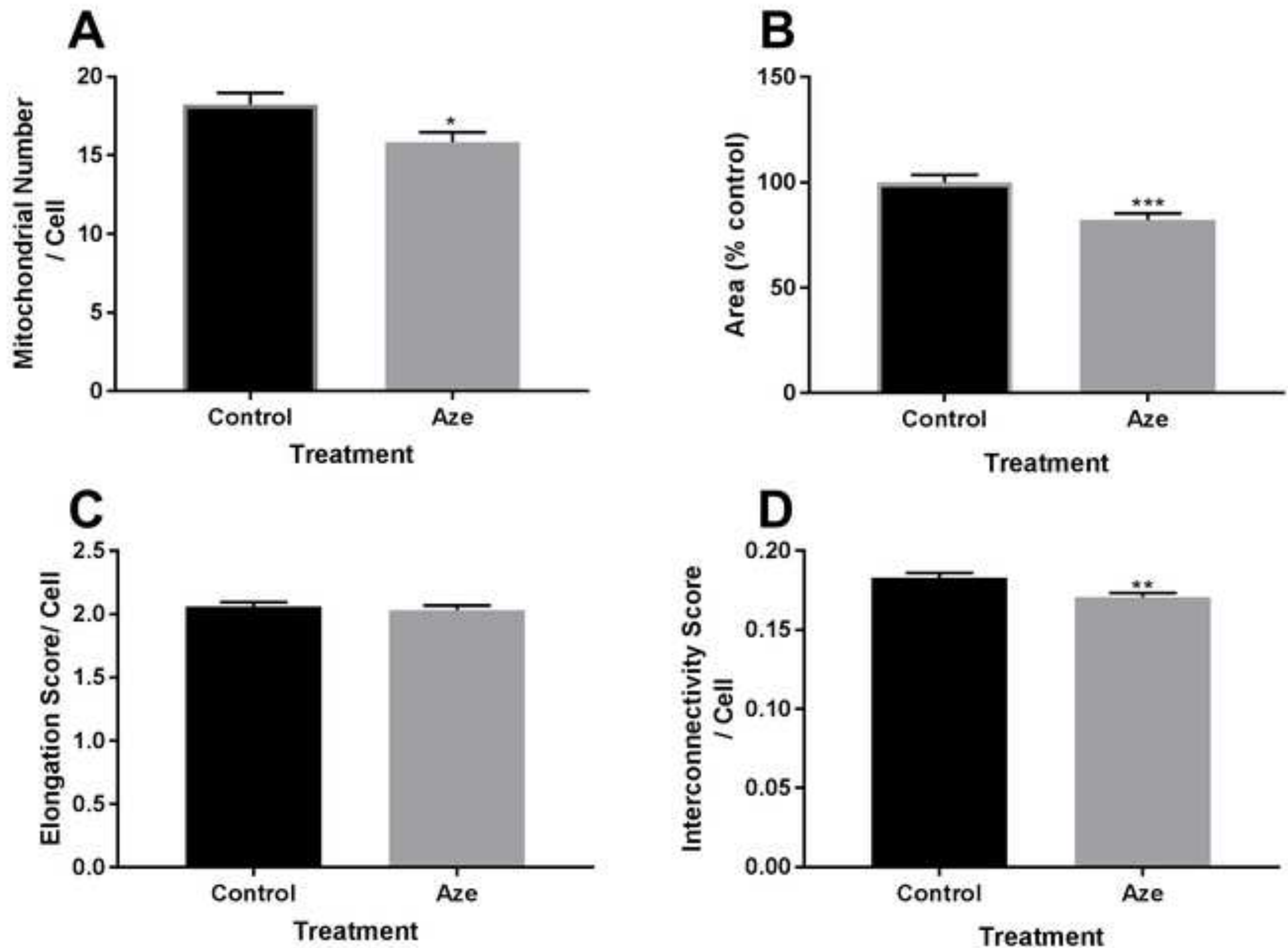

 Click here to access/download;Figure;Fig 5 Aze.tif